

Ferrimagnetic and metamagnetic layered cobalt(II)-hydroxides: first observation of a coercive field greater than 5 T

BY M. KURMOO

*Institut de Physique, Chimie et Matériaux de Strasbourg,
23 rue du Loess, 67037 Strasbourg Cedex, France*

The synthesis, characterization by XRD, UV-vis, IR and TGA and the magnetic properties of four layered compounds, namely

- 1** $\text{Co}_5(\text{OH})_8(\text{H}_2\text{O})_2(\text{NO}_3)_2$;
- 2** $\text{Co}_5(\text{OH})_8(\text{O}_2\text{CC}_6\text{H}_4\text{CO}_2) \cdot 2\text{H}_2\text{O}$;
- 3** $\text{Co}_2(\text{OH})_3(\text{NO}_3)$;
- 4** $\text{Co}_4(\text{OH})_2(\text{O}_2\text{CC}_6\text{H}_4\text{CO}_2)_3 \cdot (\text{NH}_3)_{1.5}(\text{H}_2\text{O})_{2.5}$,

are reported. **1** and **2** are characterized by triple-deck layers consisting of both octahedral and tetrahedral cobaltous ions and **3** and **4** contain single-deck layers of only octahedral cobaltous ions. **1** and **2** behave as ferrimagnets which are characterized by a minimum in the χT versus T plot, spontaneous magnetization, imaginary AC-susceptibility and hysteresis loop. The Curie temperatures are 30 and 40 K and the coercive fields at 4.2 K are 850 and 1750 Oe, respectively. **3** and **4** behave as metamagnets which are characterized by maxima in the susceptibility at the Néel temperature of 10 and 38 K, respectively, and by a critical field (antiferromagnetic \leftrightarrow paramagnetic) of *ca.* 1 kOe for **3** at 4.5 K and greater than 50 kOe for **4** at 2 K. The tricritical temperature, separating the region of reversible and non-reversible M versus H , for **4** is established at 22.5 K. The long-range magnetic ordering for the two structural types is discussed on the basis of dipolar interactions between layers. The intralayer interactions are ferromagnetic in all cases whereas the interlayer interactions are ferromagnetic for **1** and **2** and antiferromagnetic for **3** and **4**. The results indicate that the Curie or Néel temperature is weakly dependent on the interlayer distance and its observation does not depend on the existence of covalent bonds between the layers. The large coercive fields observed are due to the alignment of the moments perpendicular to the layers and the synergy between crystalline shape and single-ion anisotropies.

Keywords: cobalt; magnet; layer; clay; hydroxide

1. Introduction

Among the many infinite assemblies of magnetic moments relevant to magnetism, those consisting of two-dimensional arrays are of particular importance (De Jongh 1990; Kahn 1993; Heinrich & Bland 1994). An important commercial demand is

alignment of moments perpendicular to the layers, a feature of great value for magnetic recording devices with high-density information-storage capacity (Andrä *et al.* 1991). This class of materials also invites interesting theoretical and experimental questions (De Jongh 1990). One of the first is the existence of long-range ordering for two-dimensional Heisenberg systems. Spin-frustration in triangular lattices is another issue. Due to the existence of weak interlayer interactions through van der Waal or hydrogen bonds and via dipolar through space, an important question often asked is 'when can a crystalline material be classified as two dimensional'. These fundamental questions have consequently stimulated an enormous amount of study in the last twenty years (De Jongh & Miedma 1974; De Jongh 1990; Kahn 1996). From a chemical point of view they are additionally attractive as one is able to conserve the structure within the two-dimensional sheets and systematically tune that in the third dimension (Schollhorn 1984; Mitchell 1990; Clearfield 1991; Jacobsen 1992; O'Hare 1993; Meyn *et al.* 1993; Carlino 1997; Newman & Jones 1998).

From a magnetic point of view the problem is reduced to one dimension as principally the interlayer magnetic exchange interactions are modified. Such studies have been documented for several families of molecular compounds which include: (a) the layered perovskite, A_2MX_4 , where A is an alkali metal or an alkyl- or aryl-ammonium and M is Cu^{II} (Miedema *et al.* 1963; De Jongh *et al.* 1969) or Cr^{II} (Fair *et al.* 1977; Bellitto & Day 1992; Day 1997); (b) the heterometallic layered oxalates, $AM^{II}M^{III}(C_2O_4)_3$ (Tamaki *et al.* 1992*a,b*; Atovmyan *et al.* 1993; Mathonière *et al.* 1996; Carling *et al.* 1996; Clemente-Leon *et al.* 1997; Day 1997; Decurtins *et al.* 1998; Nuttall & Day 1998); and (c) the metal dihalides (Schieber 1967; Day 1988; Aruga Katori *et al.* 1996) having the $CdCl_2$ or CdI_2 structure (Wells 1984) and some phosphates (Carling *et al.* 1995; Bellitto *et al.* 1998; Fanucci *et al.* 1998) of divalent metals. The first class is ferromagnetic due to the orthogonal alignment of the magnetic orbitals brought about by the Jahn–Teller distortion for metals with d^4 and d^9 electronic configurations. The second class are either ferromagnetic or ferrimagnetic due to uncompensated moments between the two sublattices (M^{II} and M^{III}) of the honeycomb structure. Compounds of the third class are antiferromagnets except for a few cases of canting. Similar behaviour has been reported for the phosphates.

Recent observations of long-range magnetic ordering in the series of transition metal hydroxides (Rabu *et al.* 1993; Fujita & Awaga 1996; Rouba 1996; Laget *et al.* 1998; Kurmoo *et al.* 1999) and the high level of magnetic hardness (Kurmoo *et al.* 1999) in the cobalt compounds prompted us to explore these systems further, on the one hand, by tuning the interlayer spacing and, on the other, by inserting electronically or optically active molecules or ions in the galleries to generate dual-property (electronic–magnetic or magneto-optic) compounds (Kurmoo *et al.* 1995; Nicoud 1994). The possibility of inserting neutral and charged species is also appealing since one is able to tune the magnetic interactions by electrostatic means. There are some controversial reports regarding the types of long-range ordering for these systems; for instance, for the copper(II) compounds ferromagnetic (Laget *et al.* 1998), antiferromagnetic and weak ferromagnetic ground states (Fujita & Awaga 1996) have been proposed. For the cobalt compounds the multiphase nature and the lack of structural data have hampered development. In an attempt to clarify some of these questions, we have developed layered metal hydroxides with a range of anions having different coordinating groups, such as alkyl- or aryl-carboxylates, -dicarboxylates, -sulphonates (Kurmoo *et al.* 1999), -sulphates, and also polycyanide anions such as

dicyanamide and tricyanomethanide. In this paper, we present the characterization and the magnetic results of two structural types of cobalt compounds, one having only octahedral sites and the other containing both octahedral and tetrahedral sites. In each structural type we have employed the nitrate and the terephthalate ions; the second can provide covalently bonded bridges (Burrows *et al.* 1997; Cano *et al.* 1997; Cotton *et al.* 1998; Fogg *et al.* 1998*a,b*; Li *et al.* 1998) between the layers.

For cobalt hydroxide materials with nitrate as an anion three compounds have been reported: $\text{Co}(\text{OH})(\text{NO}_3)$ is a pink double chain compound (Rouba 1996), whereas $\text{Co}_2(\text{OH})_3(\text{NO}_3)$ and $\text{Co}_7(\text{OH})_{12}(\text{NO}_3)_2$ are pink and green layered compounds (Laget *et al.* 1996), respectively. The structures of the latter two are thought to be built up of brucite, $\text{Mg}(\text{OH})_2$, layers. The first two are reported to behave as metamagnets and the third as a ferromagnet (Laget *et al.* 1996). In a systematic study, we have recently (Kurmoo *et al.* 1999) shown that it is possible to create pillared clay-like compounds by using long-chain alkyl sulphonates using exchange for the copper salt and a one-pot synthesis for the cobalt and nickel. The copper compound, $\text{Cu}_2(\text{OH})_3\text{C}_{12}\text{H}_{25}\text{SO}_3 \cdot \text{H}_2\text{O}$, exhibits short-range antiferromagnetic interactions; the nickel compound, $\text{Ni}_2(\text{OH})_3\text{C}_{12}\text{H}_{25}\text{SO}_3 \cdot \text{H}_2\text{O}$, is a ferromagnet ($T_C = 18$ K, coercive field is 400 Oe at 4.2 K); and the cobalt compound, $\text{Co}_5(\text{OH})_8(\text{C}_{12}\text{H}_{25}\text{SO}_3)_2 \cdot 5\text{H}_2\text{O}$, is a ferrimagnet ($T_C = 50$ K, coercive field is 19 000 Oe at 2 K). The most unusual result in this series is the observation of long-range magnetic ordering for metal layers separated by as much as 25 Å. The long-range magnetic ordering at such a high temperature was explained by a dipolar mechanism (Drillon & Panissod 1998) whereby the correlation length in the layer diverges as the Curie temperature is approached from above, resulting in clusters with large effective spin which interact via dipolar interactions. Furthermore, the wide hysteresis loop classifies $\text{Co}_5(\text{OH})_8(\text{C}_{12}\text{H}_{25}\text{SO}_3)_2 \cdot 5\text{H}_2\text{O}$ as one of the hardest metal-organic magnets known (Kurmoo & Kepert 1998). The magnetic hardness results from the alignment of the moments perpendicular to the layers and the synergy of crystalline shape and single-ion anisotropies (Chikazumi 1978).

One particular objective for this study was to establish the magnetic ground states of the different structural types of cobalt layers. The second point was to understand the role of the bridging ligand on the exchange interactions. It is anticipated that such studies may shed some light on the confusion regarding the various magnetic ground states reported. Therefore, we have reinvestigated the nitrate-containing compounds and report an extensive magnetic study of $\text{Co}_2(\text{OH})_3(\text{NO}_3)$ and of a novel phase, $\text{Co}_5(\text{OH})_8(\text{H}_2\text{O})_2(\text{NO}_3)_2$. We also present the results of two new compounds, $\text{Co}_4(\text{OH})_2(\text{O}_2\text{CC}_6\text{H}_4\text{CO}_2)_3 \cdot (\text{NH}_3)_{1.5}(\text{H}_2\text{O})_{2.5}$ and $\text{Co}_5(\text{OH})_8(\text{O}_2\text{CC}_6\text{H}_4\text{CO}_2) \cdot 2\text{H}_2\text{O}$ containing bridging terephthalate.

2. Experimental section

(a) Syntheses

$\text{Co}_5(\text{OH})_8(\text{H}_2\text{O})_2(\text{NO}_3)_2$, **1**, was obtained as a bright green powder by adding 3 ml of aqueous ammonia (30%) drop by drop to a warm (40 °C) solution of $\text{Co}(\text{H}_2\text{O})_6(\text{NO}_3)_2$ (3 g) and NaNO_3 (3 g) in 250 ml of a 1:1 mixture of water and absolute ethanol. The precipitate was filtered, washed and dried in air. Yield: 1.0 g.

For $\text{Co}_5(\text{OH})_8(\text{O}_2\text{CC}_6\text{H}_4\text{CO}_2) \cdot 2\text{H}_2\text{O}$, **2**, a procedure similar to that described above for **1** was employed, using terephthalic acid (1 g) in the place of the sodium nitrate. Yield: 1.1 g.

$\text{Co}_2(\text{OH})_3(\text{NO}_3)$, **3**, was prepared as a pink solid by a slight modification to a procedure reported previously (Rouba 1996): a solution of NaOH (1.2 g in 20 ml of water) was added, drop by drop, to a refluxing solution of $\text{Co}(\text{H}_2\text{O})_6(\text{NO}_3)_2$ (5.8 g in 20 ml of water) under a flow of argon for 24 h. The precipitate was washed with cold water and acetone and air dried. Yield: 2.1 g.

$\text{Co}_4(\text{OH})_2(\text{O}_2\text{CC}_6\text{H}_4\text{CO}_2)_3 \cdot (\text{NH}_3)_{1.5}(\text{H}_2\text{O})_{2.5}$, **4**, was prepared by mixing $\text{Co}(\text{H}_2\text{O})_6(\text{NO}_3)_2$ (3 g), terephthalic acid (1 g) and 3 ml of aqueous ammonia (30%) in a warm (40°C) solution of 250 ml of water and absolute ethanol (1:1 mixture). A blue green precipitate was produced which was transformed into the titled compound by reducing the solution volume to 60 ml at 80°C. The pale pink powder was washed with water, ethanol and dried in air. Yield: 1.1 g.

The compositions of the compounds were confirmed by chemical and thermogravimetric analyses.

(b) Thermogravimetric analyses

Data were collected in the temperature range 20–1100 °C by warming the sample at a rate of 6 °C min⁻¹ in air on a SETARAM TGA 92 calorimeter.

(c) X-ray diffraction

X-ray powder diffraction were recorded at room temperature on a SIEMENS D500 diffractometer employing Co- $K\alpha 1$ (1.789 Å) and a flat plate geometry. Data were recorded in the 2θ range from 2–72° with a step of 0.02°.

(d) Infrared and UV-vis spectroscopies

Infrared spectra were obtained from fine powder of the compounds dispersed onto a KBr plate with the use of a MATTSON FTIR spectrometer. UV-vis spectra were recorded in the range 300–900 nm by transmission through thin films of the compounds dispersed in paraffin oil. The scattering due to the powdered samples was compensated by a piece of tissue paper soaked with the oil and placed in the reference beam.

(e) Magnetic properties

(i) Faraday balance

The temperature-dependence (4–300 K) of the magnetization of each sample was measured on a home-built Faraday-type pendulum in a field up to 13 000 Oe. The temperature of the sample in the continuous flow cryostat was controlled by either an Oxford Instruments ITC4 or a BT 400. The sample was held in a gelatine capsule and the data were corrected for its diamagnetism and those of the atomic diamagnetism using Pascal's constants.

(ii) *SQUID*

The temperature (2–300 K) and field (up to 5 T) dependence of the magnetization of the samples were recorded on a MPMS-XL magnetometer. AC susceptibilities were measured on the same instrument in a field of 1 Oe oscillating at 20 Hz. The samples were held in gelatine capsules. For hysteresis measurements in high field the samples were fixed in the capsules to prevent rotation. Any special protocol of each experiment is detailed in the relevant section.

(iii) *Vibrating sample magnetometer*

Isothermal magnetization of the compounds was recorded at several temperatures ($T > 4.2$ K) in fields up to ± 1.8 T by use of a Princeton Applied Research Model 155. The temperature of the sample in a bath cryostat was controlled by an Oxford Instruments ITC4. Samples were mounted in 5 mm diameter perspex containers.

3. Results and discussion

Before describing the results it is worthwhile for the understanding of this paper to give a basic description of metamagnetism (Herpin 1968), for it is rarely observed. Furthermore, the large coercive field exhibited by the metamagnet, **4**, described below, opens up a new class of magnetic materials. A metamagnet is an antiferromagnet with strong anisotropy. Below T_N , application of a magnetic field along the easy axis reverses the moments to the parallel orientation without passing through a spin-flop state and resulting in a paramagnetic state. Strong correlation between the moments is thought to create domains which give rise to hysteresis, in some cases, below a tricritical or a bicritical end-point temperature (Stryjewski & Giordano 1977). Metamagnetism is usually observed in layered compounds, where there exists a strong structural anisotropy and, consequently, anisotropy in and competitions between the exchange interactions. Some of the most studied compounds are the halides (Cl, Br and I) (Stryjewski & Giordano 1977; Aruga Katori & Katsumata 1996; Day 1988; Schieber 1967) and hydroxides (Takada *et al.* 1966*a, b*) of the divalent iron group ions. They adopt the CdI_2 or CdCl_2 structure with strong covalent bonds within the layer and weak hydrogen bonds between layers (Wells 1984). The nearest-neighbour intralayer exchange interactions between metals are ferromagnetic and interlayer interactions are antiferromagnetic and generally, dipolar in nature (Stryjewski & Giordano 1977). It has been demonstrated, experimentally and theoretically, that when the easy axis is perpendicular to the layers (e.g. FeCl_2), hysteresis is more pronounced than when it is parallel (e.g. CoCl_2 and NiCl_2). Therefore, FeCl_2 behaves, in some ways, like a ferromagnet with domains and CoCl_2 and NiCl_2 behave as paramagnets.

(a) *Syntheses*

The synthesis of a particular phase depends on the choice of transition metals: copper and nickel behave differently to cobalt due to the fact that copper and nickel adopt only octahedral geometry, whereas cobalt atoms can have either only octahedral geometry or both octahedral and tetrahedral geometries. The pertinent reaction

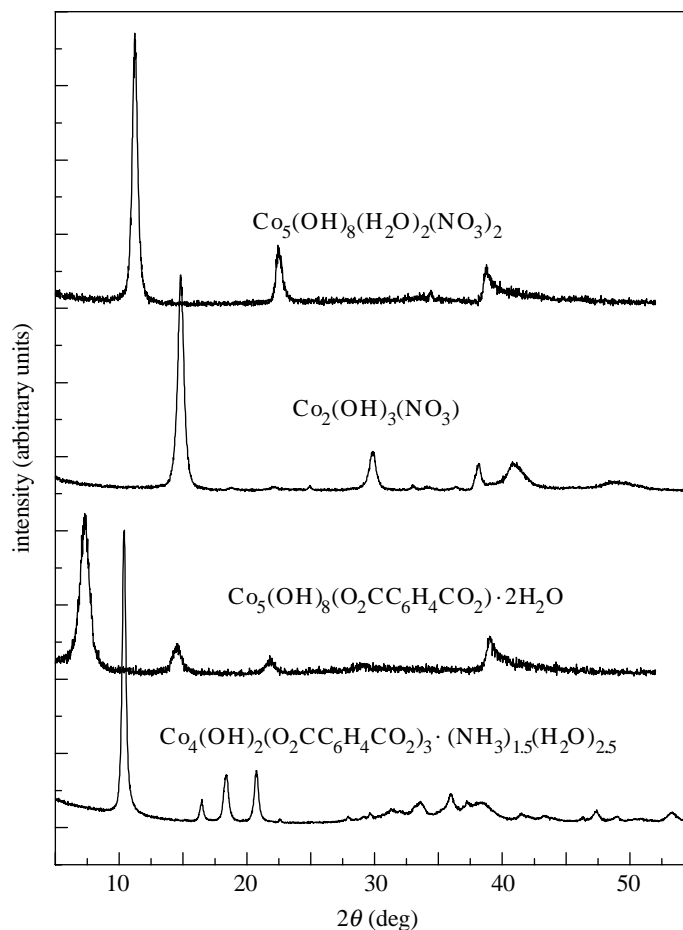
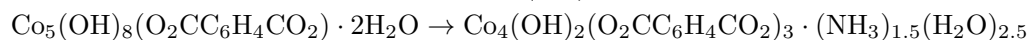
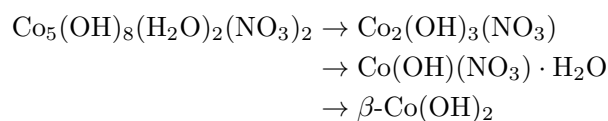


Figure 1. Powder X-ray diffraction of **1**, **2**, **3** and **4** (Co- $K\alpha$, $\lambda = 1.789 \text{ \AA}$).

conditions depend on the concentration of the ions and the pK_a of the anions. For cobalt, the reactions with nitrate and terephthalate proceed as follows:



(b) *X-ray diffraction*

The X-ray diffraction patterns of the four compounds are shown in figure 1. **1** and **2** display only a progression of the $00l$ in their diffraction patterns and two broad features at d-spacing of 2.70 and 1.55 \AA . As mentioned in the introduction, the structures of these compounds are related to those observed for monoclinic $\text{Zn}_5(\text{OH})_8(\text{H}_2\text{O})_2(\text{NO}_3)_2$ (Stählin & Oswald 1970) and hexagonal $\text{Zn}_5(\text{OH})_8\text{Cl}_2 \cdot \text{H}_2\text{O}$ (Allmann 1968). However, the available information is not enough to differentiate

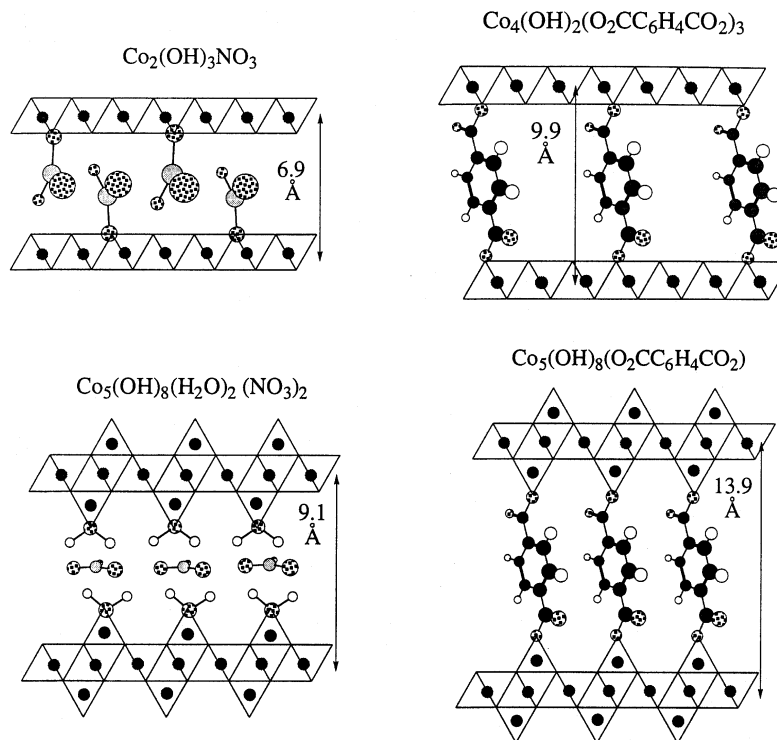


Figure 2. Idealized single-decker layer structures for **2** and **4** and triple-layer structures for **1** and **3** showing a single layer of octahedral cobalt sandwiched by two layers of tetrahedral cobalt and the terephthalate in a bridging position.

between the two possibilities. The interlayer separation of 9.14 Å for **1** and the infrared data (*vide supra*) suggest that the nitrate is not bonded to the cobalt. The 13.87 Å spacing for **2** is as expected for a terephthalate di-anion acting as a bridge between two layers (Burrows *et al.* 1997; Newman & Jones 1998; Cano *et al.* 1997; Cotton *et al.* 1998; Fogg *et al.* 1998b). The calculated distance between the two oxygen atoms of the two carboxylate groups is 7.4 Å, giving a thickness of 6.5 Å for the inorganic triple-deck layer. This value can be compared to an estimation of 3 Å for the pink single-deck layered compounds. A unique set of unit-cell parameters for **3** was found using TREOR (Werner *et al.* 1985) and they were refined within the pattern matching module of FULLPROF (Rodriguez-Carvajal 1997) to give $a = 5.53(1)$, $b = 6.31(1)$, $c = 6.95(1)$ Å, $\beta = 93.1^\circ$, $V = 242$ Å³, which are in good agreement with those in the literature (Rouba 1996). Similar procedures give $a = 9.97(1)$, $b = 11.24(1)$, $c = 6.29(1)$ Å, $\beta = 95.95^\circ$ for **4**. The a parameter corresponds to the interlayer separation, the b parameter to $4r \sin \frac{1}{3}\pi$ and the c parameter to $2r$, where r is the Co–Co distance (3.15 Å). The magnitude of the a parameter is in agreement with the sum of two Co–O bonds (*ca.* 2 Å) and the distance (7.4 Å) between terminal oxygen atoms of the terephthalate and angle β of 96° . The idealized structures based on the structures of $\text{Mg}(\text{OH})_2$ and $\text{Zn}_5(\text{OH})_8(\text{H}_2\text{O})_2(\text{NO}_3)_2$ for the nitrate and terephthalate compounds are shown in figure 2.

Table 1. *Energies and intensities of bands observed in the infrared spectra of 1, 2, 3 and 4*

compound	observed band energy (cm ⁻¹)
1 Co ₅ (OH) ₈ (H ₂ O) ₂ (NO ₃) ₂	511m, 659m, 832vw, 879w, 1370vs, 1476sh, 1615w, 3455s br
2 Co ₅ (OH) ₈ (O ₂ CC ₆ H ₄ CO ₂) ₃ · 2H ₂ O	513m, 656m, 749m, 815m, 1359s, 1392sh, 1501m, 1585s, 3330sh, 3470br
3 Co ₂ (OH) ₃ (NO ₃)	500w, 633s, 689s, 726s, 804m, 1001m, 1313s, 1487s, 3580s, 3612sh
4 Co ₄ (OH) ₂ (O ₂ CC ₆ H ₄ CO ₂) ₃ · (NH ₃) _{1.5} (H ₂ O) _{2.5}	515m, 743s, 807s, 1015w, 1359s, 1392sh, 1498m, 1577s, 1705w, 3140br, 3500br

(c) Infrared

The energies and intensities of the observed bands are listed in table 1. The bands at low energy (less than 800 cm⁻¹) are assigned to the bending mode M—O—H (Nakamoto 1986) and those at high energy (greater than 2500 cm⁻¹) are assigned to the C—H and O—H stretching modes. Compounds containing the water molecules, either coordinated or as solvent, show the bending mode of water at *ca.* 1600 cm⁻¹. The intermediate energy bands are those of the anions, NO₃ and terephthalate (Stählin & Oswald 1971; Zotov *et al.* 1990).

The free nitrate ion adopts the *D*_{3h} point group and on coordination its symmetry is lowered. Consequently, the totally symmetric mode at 1050 cm⁻¹ becomes IR active. Furthermore, the position of this band changes according to its mode of coordination; for unidentate complexes (local point group *C*_{2v}) it is expected at *ca.* 1000 cm⁻¹ and for bidentate chelation it moves to *ca.* 1025 cm⁻¹. The observation of this band at 1001 cm⁻¹ in **3** suggests that the nitrate has a unidentate coordination to the cobalt, in agreement with the proposed crystal structure (figure 2). In **1**, on the other hand, the weakness of this band and the observation of a strong central band at 1370 cm⁻¹ suggest that the nitrate ion is not coordinated. In this case the water molecules must bind to the metal to satisfy the coordination number and charge. A similar structure is observed for Zn₅(OH)₈(H₂O)₂(NO₃)₂, where the water molecules make the coordination (Stählin & Oswald 1970).

The two terephthalate compounds show two strong bands at *ca.* 1360 and *ca.* 1580 cm⁻¹, which are assigned to the antisymmetric and symmetric stretching modes of the carboxylate group, respectively. The energy difference between these two bands suggests that the carboxylate groups are unidentate (Nakamoto 1986). Observation of only one band of each suggests that the two carboxylate ends of the terephthalate are equivalent, confirming that the anion bridges the cobalt atoms of adjacent layers in both compounds.

(d) UV-vis

The UV-vis spectra of the compounds are shown in figure 3 and energies and assignments (Lever 1986) of the observed bands are given in table 2. The two types

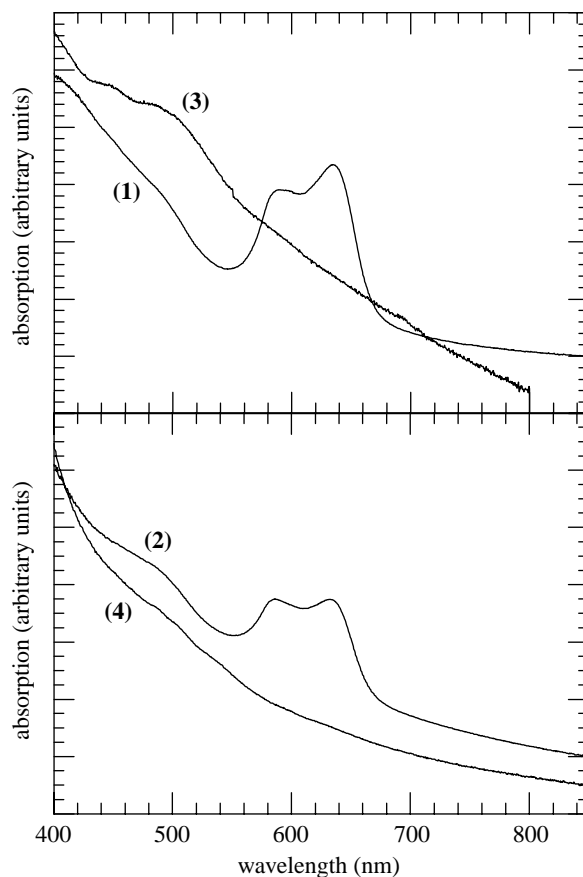

 Figure 3. Transmission UV-vis electronic absorption spectra of **1**, **2**, **3** and **4**.

 Table 2. Energies and assignments of bands observed in the UV-vis spectra of **1**, **2**, **3** and **4**

compound	transition energy (cm ⁻¹)	assignment
1 Co ₅ (OH) ₈ (H ₂ O) ₂ (NO ₃) ₂	15 800	⁴ A ₂ → ⁴ T ₁ (P)
	17 000	⁴ T _{1g} (F) → ⁴ A _{2g} (P)
	20 300	⁴ T _{1g} (F) → ⁴ T _{1g} (P)
2 Co ₅ (OH) ₈ (O ₂ CC ₆ H ₄ CO ₂) · 2H ₂ O	15 800	⁴ A ₂ → ⁴ T ₁ (P)
	17 000	⁴ T _{1g} (F) → ⁴ A _{2g} (P)
	21 800	⁴ T _{1g} (F) → ⁴ T _{1g} (P)
3 Co ₂ (OH) ₃ (NO ₃)	19 800	⁴ T _{1g} (F) → ⁴ A _{2g} (P)
	22 500	⁴ T _{1g} (F) → ⁴ T _{1g} (P)
4 Co ₄ (OH) ₂ (O ₂ CC ₆ H ₄ CO ₂) ₃ · (NH ₃) _{1.5} (H ₂ O) _{2.5}	20 000 weak and broad	{ ⁴ T _{1g} (F) → ⁴ A _{2g} (P) ⁴ T _{1g} (F) → ⁴ T _{1g} (P)

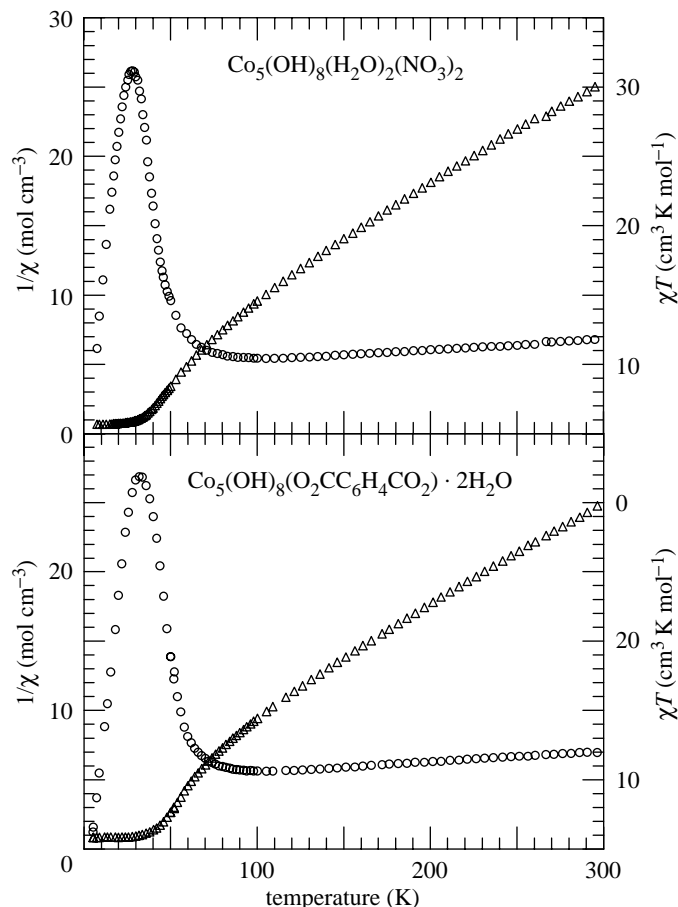


Figure 4. Temperature dependence of the inverse DC susceptibilities (triangles) and the products susceptibility and temperature (circles) of **1** and **2** in an applied field of 13 000 Oe.

of compounds are quite distinct; the pink compounds show weak d–d absorption corresponding to Co(II) in octahedral coordination of a weak ligand and the green compounds show two additional sharp peaks at lower energies corresponding to Co(II) in tetrahedral coordination geometry.

(e) *Magnetic properties*

For **1** and **2** The temperature dependence of the inverse magnetic susceptibilities and the products of susceptibility and temperature [$\chi(T - \Theta) = C$] of the two compounds are shown in figure 4. The magnetic behaviour of the two compounds is identical. The high-temperature ($T > 150$ K) data fit the Curie–Weiss law with Curie constants of 13.42(5) and 13.3(1) $\text{cm}^3 \text{K mol}^{-1}$, and Weiss temperatures of $-37(1)$ and $-40(2)$ K, respectively. The Curie values are consistent with that expected for the sum of three octahedral and two tetrahedral divalent high-spin cobalt atoms. The effective moment shows a minimum at 110 K, suggesting ferrimagnetic behaviour and a maximum at *ca.* 30 K. The latter is due to saturation since the measurements were made in 13 kOe. We should emphasize that the value of the moment at the maximum

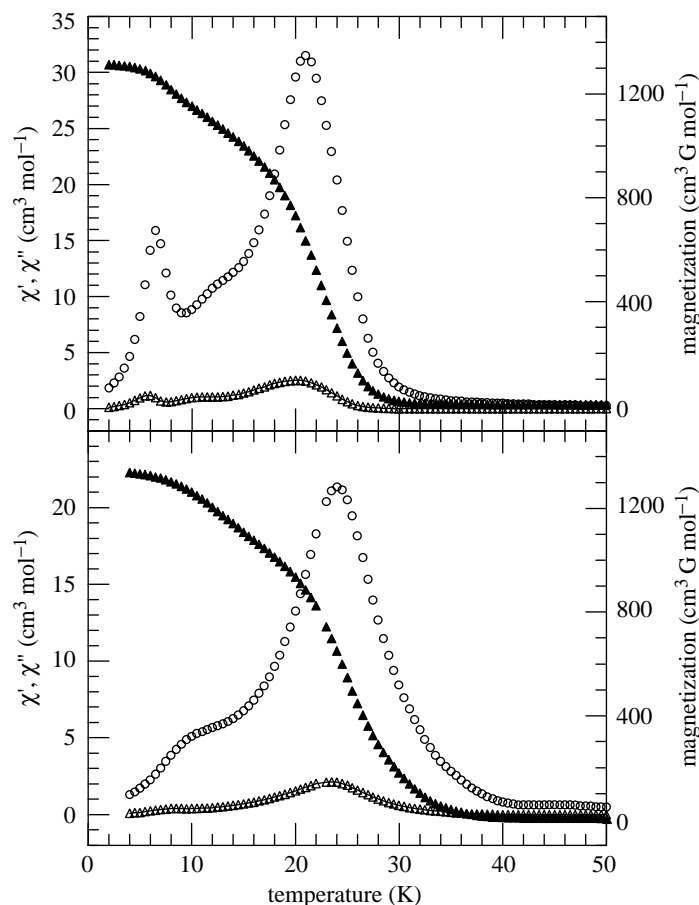


Figure 5. Temperature dependence of the DC magnetization (filled triangles) in a field of 1 Oe and the real (open circles) and imaginary (open triangles) AC susceptibilities in a field of 1 Oe for **1** (top) and **2** (bottom).

in any given field has no real information (Laget *et al.* 1998) because it is dependent on the applied field.

The Curie temperatures were obtained by measuring the magnetization on cooling in a small applied field of 1 Oe and by the onset of the imaginary component of the AC susceptibility. The transitions are quite broad (figure 5), possibly due to the two-dimensional nature of these compounds (De Jongh 1990). The Curie temperatures are 30(3) and 40(3) K for **1** and **2**, respectively. In contrast to the smooth temperature dependence of the magnetization data in the high field, the low-field DC data and, in particular, the AC data exhibit several features. These may be due to a minor impurity phase in the samples. For the nitrate salt, the sharp peak in χ' and its associated χ'' suggest that the minor phase is also magnetic. A closer look at the XRD does not reveal any other weak features, whereas the infrared data contains a weak shoulder at 1476 cm^{-1} which may be interpreted as arising from a coordinated nitrate in the minor phase. We should point out that in the zinc analogues, an example with coordinated ammonia $\text{Zn}_5(\text{OH})_8(\text{NH}_3)_2(\text{NO}_3)_2$ is known (Louer *et al.*

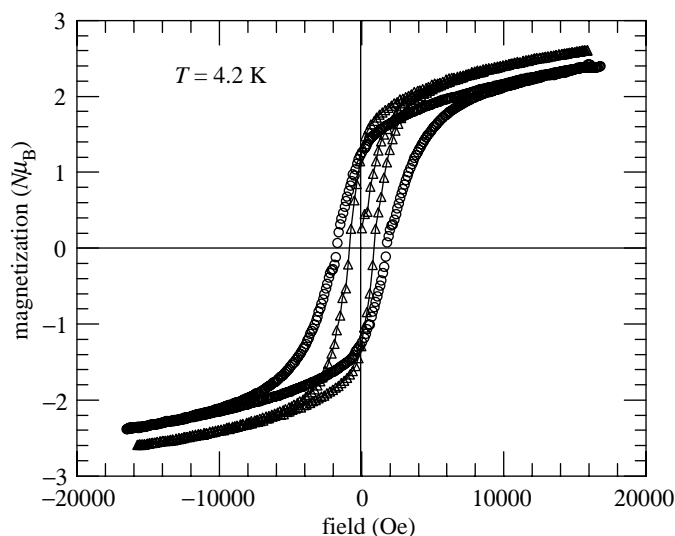


Figure 6. Isothermal magnetization at 4.2 K for **1** (triangles) and **2** (circles).

1973; Benard *et al.* 1994). Chemical analyses and the infrared data of our compounds reveal the absence of ammonia.

The isothermal magnetization of **1** and **2** at 4.2 K is shown in figure 6. Both compounds exhibit hysteresis loops with the coercive field increasing with lowering temperature and reaching 850 and 1750 Oe at 4.2 K, respectively. The remanent magnetization, after applying a field of 18 000 Oe, has almost the same temperature dependence as the magnetization in a small field of 1 Oe, reaching zero at the Curie temperatures. The values of the magnetization at 4.2 K in a field of 18 000 Oe are marginally lower than $3\mu_B$, the value expected for a ferrimagnet with one sublattice consisting of three cobalt(II) and another of two cobalt(II).

For **3** The temperature dependence of the magnetic susceptibility in different applied magnetic fields is shown in figure 7. The susceptibility increases as the temperature of the sample is lowered according to a Curie–Weiss law with Curie and Weiss constants of $6.11(1) \text{ cm}^3 \text{ K mol}^{-1}$ and $+8.6(3) \text{ K}$, respectively, suggesting ferromagnetic short-range interaction between nearest cobalt neighbours. The Curie constant is less than that reported previously (Rabu *et al.* 1993) and is within the range expected for octahedral cobaltous ion (Figgis 1966). Below 20 K nonlinear susceptibility behaviour is observed. In a small applied field (less than 1000 Oe), the susceptibility decreases below 10 K and tends toward half the value at the maximum, a behaviour consistent with antiferromagnetic long-range ordering. In an applied field of 3200 Oe, the susceptibility increases continuously. In applied fields in excess of 5000 Oe the susceptibility is lowered due to saturation effects. The isothermal magnetization at 4.5 K is shown in figure 9. The magnetization increases slowly in the low field and above a critical field of *ca.* 1000 Oe it increases more rapidly before reaching a plateau at $3.2\mu_B$ in a field of 16 000 Oe. There is a very slight hysteresis of 100 ± 50 Oe around the critical field.

For **4** the magnetic susceptibility is field dependent as in the case of **3**. In a small applied field of 10 Oe it increases to a maximum at T_N (38 K) and in a field 5000 Oe, larger than the critical field, it increases to a saturation plateau (fig-

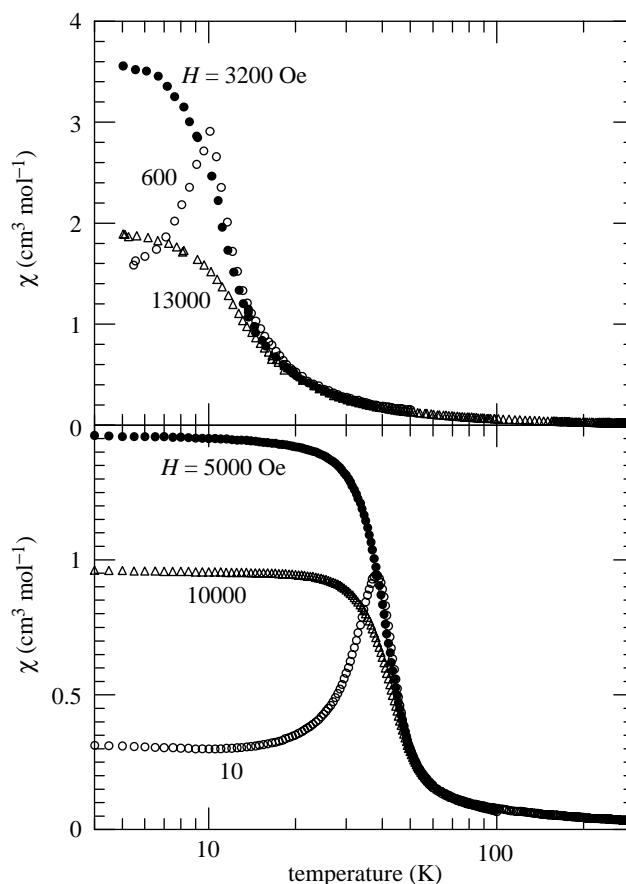


Figure 7. Temperature dependence of the DC magnetization for **3** (top) and **4** (bottom).

ure 7). The Curie constant derived from a Curie–Weiss fit of the inverse susceptibility versus temperature for the low-field data and for $T > 150$ K gives $C = 11.86(3) \text{ cm}^3 \text{ K mol}^{-1}$ and $\Theta = -67(1) \text{ K}$. The Curie constant, $2.97 \text{ cm}^3 \text{ K}$ per mole cobalt ($\mu_{\text{eff}} = 4.87\mu_{\text{B}}/\text{cobalt}$), is in good agreement to that expected for octahedral cobalt(II). The product of susceptibility and temperature, which is the square of the effective moment, decreases on lowering temperature to a minimum at 90 K and peaks at T_{N} at a value three times that at room temperature. The decrease from high temperature to 90 K is due to the effect of spin-orbit coupling (Mabbs & Machin 1973) resulting from an increasing population of the $s = \frac{1}{2}$ state at low temperatures, followed by an increase due to short-range ferromagnetic interactions between the cobalt atoms within the layer becoming more important than spin-orbit coupling. At 38 K, long-range ordering sets in due to antiferromagnetic interactions between moments in adjacent layers (Nagamiya *et al.* 1955). In a field higher than the anisotropy field, the moments are forced to be parallel.

The AC susceptibility in an applied AC field of 1 Oe is shown in figure 8. The real part shows a peak of magnitude similar to that observed for a low DC field and no anomalies are observed for the imaginary component, as expected for antiferromagnetic compounds (Goodenough 1963).

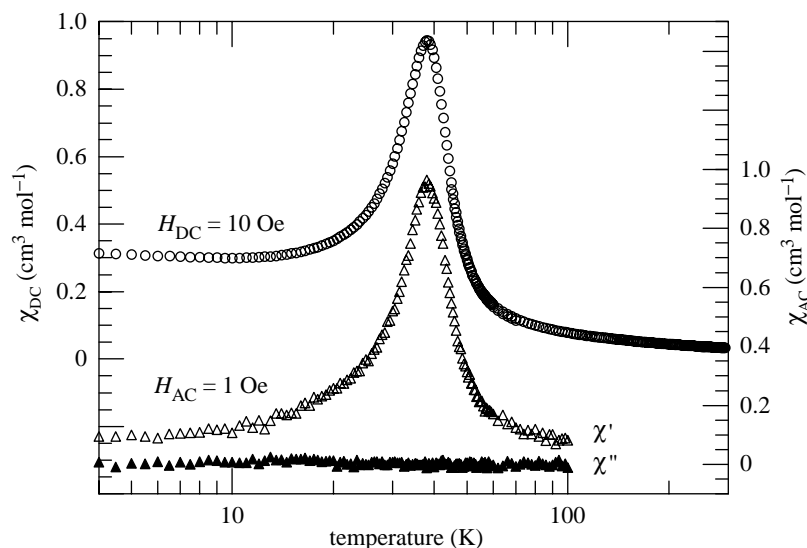


Figure 8. Temperature dependence of the DC susceptibility (open circles) and the real (open triangles) and imaginary (filled triangles) AC susceptibilities in a field of 1 Oe for **4**.

Isothermal magnetization at several temperatures is shown in figures 9 and 10. At high temperatures ($T > T_N$) the magnetization is linear and reversible as for paramagnets, while just above T_N there is a slight curvature that is a typical signature of short-range ferromagnetic interactions. Just below T_N the magnetization takes an S-shape (figure 9) and remains reversible. The critical field to align the moments parallel increases as the temperature is lowered (figure 11). Below 22.5 K the magnetization begins to exhibit hysteresis (remanent magnetization and coercive field) and the hysteresis width increases on lowering the temperature. The shape of the loops changes gradually from the S-shape to one more commonly associated with a ferromagnet. The behaviour down to a temperature of 15 K is typical of that observed for metamagnets with very strong anisotropy and with alignment of moments perpendicular to the layers. For most of the known metamagnets the hysteresis occurs around the critical field region and the magnetization passes through zero as the field is removed, implying no remanent magnetization and no coercive field. The unusual feature of **4** is that there is a large remanent magnetization and a large coercive field (attaining in excess of 5 T at 2 K) below the tricritical temperature of 22.5 K (figure 10). The only other example which may show such an effect is NpO_2 (oxalate) (Jones & Stone 1972); unfortunately only part of the hysteresis loops was recorded. Figure 10 also show the first magnetization after zero-field cooling (ZFC) and the hysteresis loops after field cooling (FC) the sample in 5 T from 100 K to the measuring temperature. Below 10 K, if the full (± 5 T) hysteresis loop is recorded after ZFC a symmetric loop around $H = 0$ Oe is observed which has the shape known as a Rayleigh loop, also called a primary loop. This indicates that we are unable to reverse the moments with the maximum available field of our SQUID and the sample is still in the irreversible part of the first magnetization. Figure 11 presents the temperature-field phase diagram, in which the critical field to reverse the moments is estimated by the intersection of two straight lines from the opposite ends. The error bars on these points are the maximum width of the hysteresis loop or coercive

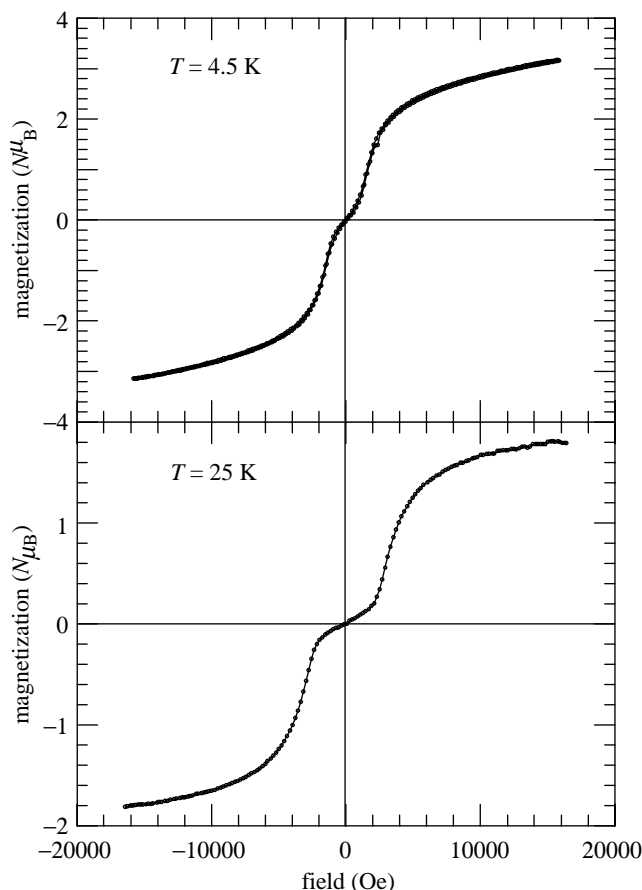


Figure 9. Isothermal magnetization for **3** at 4.5 K (top) and for **4** at 25 K.

field observed. We have also displayed the thermoremanent magnetization after field cooling in 5 T from 100 to 2 K. This is a very elegant way, in this case, to identify the tricritical point at 22.5 K.

The long-range magnetic ordering mechanism in **4** is similar to that for the ferrimagnetic systems discussed above (Kurmoo *et al.* 1999; Drillon & Panissod 1998). The only difference is that in this case the interaction is antiferromagnetic, whereas it is ferromagnetic for the triple-deck compounds. The mechanism of hysteresis for a metamagnet may be viewed as follows: cooling the sample in a very small applied field establishes antiferromagnetic ordering (figure 12) below T_N . Application of a field along the easy-axis at a temperature below T_N first reverses some of the moments, usually at some defects (nucleation sites), which then polarize their surroundings. As the field is increased the created domains increase in size until all the moments are aligned with the applied field. At the critical field the sample will contain ferromagnetic clusters embedded in the antiferromagnetic bulk. This situation is similar to the process involved in mictomagnetism. The main difference here is that the size of the domains is not decided at the manufacturing stage but is temperature dependent. At a fixed temperature, the average size of these clusters will increase with field, the effective moment of the ions and the near-neighbour exchange interac-

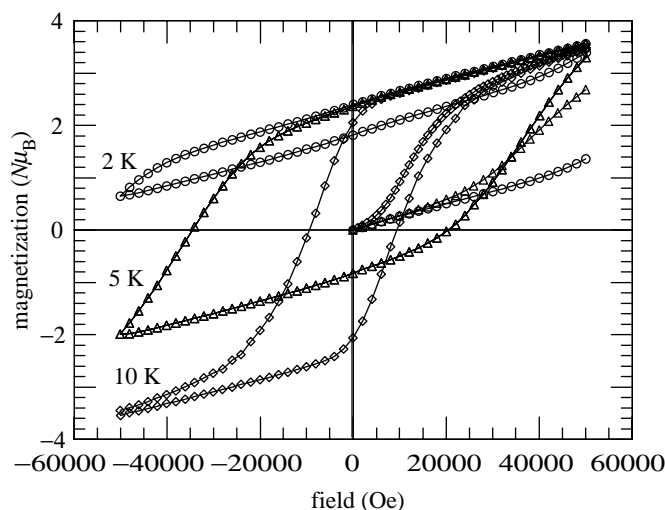


Figure 10. Isothermal first magnetization (ZFC) and hysteresis (5 T FC) loops for **4** at 2 K (circles), 5 K (triangles) and 10 K (diamonds).

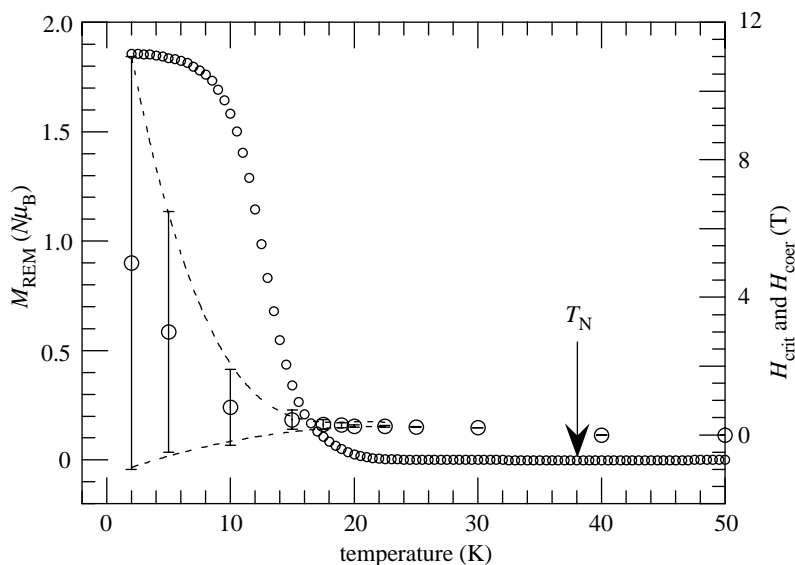


Figure 11. Field-temperature phase diagram showing the critical field (circles) and width of hysteresis (error bars) and thermoremanent magnetization for **4**. The dotted lines are guides to the eye.

tion (Chikazumi 1978). As the size becomes large the magnetocrystalline anisotropy energy is also increased and exceeds the exchange energy such that on removal of the applied field the compound retains its magnetic state and remanent magnetization and a coercive field are observed. Therefore, the critical and coercive fields will depend on the single-ion anisotropy and the magnitude of the exchange interactions. This is in contrast to that for ferromagnets or ferrimagnets where the coercive field depends solely on the single-ion anisotropy, assuming the shape is the same. To

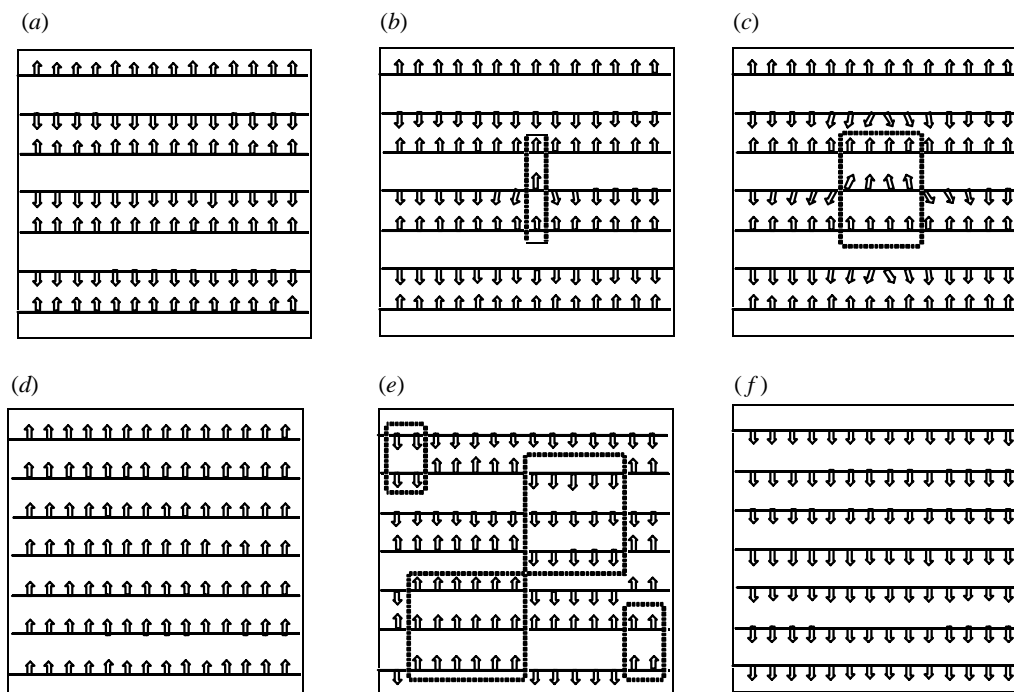


Figure 12. Schematic models of the mechanism of magnetization and demagnetization processes for **4** at a temperature below T_N after zero-field cooling. (a) $T < T_N$, $H = 0$; (b) $H = H_{\text{crit}}$; (c) $H > H_{\text{crit}}$; (d) $H \gg H_{\text{crit}}$; (e) $H = H_{\text{coer}}$; (f) $H \gg H_{\text{coer}}$.

verify this hypothesis, we have prepared cobalt–nickel solid solutions to determine the dependence of the critical and coercive fields on the magnitude of the spin-orbit coupling. Nickel substitution has two effects: first, it reduces the average moment per ion and secondly, it reduces the effective spin-orbit coupling. For the nominal Ni_2Co_2 hydroxy-terephthalate, the Néel temperature is lowered to 22 K and the coercive field to 12 000 Oe. Furthermore, the importance of dipolar interactions was verified by replacing the terephthalate ion by a longer bridging ion, 4,4'-biphenyl-dicarboxylate. Here, the interlayer spacing is increased to 14.1 Å, T_N is lowered only slightly to 34 K and the coercive field is 30 500 Oe at 5 K.

4. Conclusion

The present observations suggest that the Brucite-type layered compounds of cobalt having octahedral sites only are metamagnets, while those adopting the triple-deck $\text{Zn}_5(\text{OH})_8(\text{H}_2\text{O})_2(\text{NO}_3)_2$ structure, containing both octahedral and tetrahedral sites, are ferrimagnets. The long-range ordering in both structural types is brought about by dipolar interaction due to precursor correlation creating large effective moments in domains just above the transition temperatures. The exceptional hardness of these two structural types is due to the synergy of single-ion and crystalline shape anisotropies and, most importantly, the alignment of moments perpendicular to the layer. **4** is the first metamagnet to exhibit a coercive field and the first magnetic material which has a coercive field in excess of 5 T.

This work was funded by the CNRS-France. The technical assistance of R. Poinso and A. Derory is much appreciated. I am grateful to Dr S. Vilminot, Dr C. J. Kepert, Dr S. Blundell and Mr B. Lovett for many fruitful discussions.

References

- Allmann, R. 1968 Verfeinerung der structur des zinkhydroxidchlorids II, $Zn_5(OH)_8Cl_2 \cdot H_2O$. *Z. Kristallogr.* **126**, 417–426.
- Andrä, W., Danan, H. & Mattheis, R. 1991 Theoretical aspects of perpendicular magnetic recording media. *Physica Status Solidi* **125**, 9–55.
- Aruga Katori, H. & Katsumata, K. 1996 Specific-heat anomaly in the Ising antiferromagnet $FeBr_2$ in external magnetic fields. *Phys. Rev. B* **54**, R9620–R9623.
- Atovmyan, L., Shilov, G. V., Lyubovskaya, R. N., Zhilyaeva, E. I., Ovanesyan, N. S., Guskovskaya, I. G. & Morozov, G. 1993 Crystal structure of molecular ferromagnet $NBu_4[MnCr(C_2O_4)_3]$ (Bu = *n*-C₄H₉). *JETP Lett.* **58**, 767–769.
- Bellitto, C & Day, P. 1992 *J. Mater. Chem.* **2**, 265.
- Bellitto, C., Federici, F. & Ibrahim, S. A. 1998 Synthesis and properties of new chromium(II) organophosphonates. *Chem. Mater.* **10**, 1076–1082.
- Benard, P., Auffredic, J. P. & Louer, D. 1994 A study of the thermal decomposition of ammine zinc hydroxide nitrates. *Thermochem. Acta* **232**, 65–76.
- Burrows, A. D., Mingos, D. M. P., Lawrence, S. E., White, A. J. P. & Williams, D. J. 1997 Platinum(II) phosphine complexes of dicarboxylates and ammonia: crystal structures of $[Pt(PPh_3)_2]_2\{\mu-1,3-(O_2C)_2C_6H_4\}_2$, $[Pt(PPh_3)_2(NH_3)_2\{\mu-1,4-(O_2C)_2C_6H_4\}][PF_6]_2$ and *cis*- $[Pt(PPh_3)_2(NH_3)_2][NO_3]_2$. *J. Chem. Soc. Dalton Trans.*, pp. 1295–1300.
- Cano, J., De Munno, G., Sanz, J. L., Ruiz, R., Faus, J., Lloret, F., Julve, M. & Caneschi, A. 1997 Ability of terephthalate (ta) to mediate exchange coupling in ta-bridged copper(II), nickel(II), cobalt(II) and manganese(II) dinuclear complexes. *J. Chem. Soc. Dalton Trans.*, pp. 1915–1923.
- Carling, S. G., Day, P. & Visser, D. 1995 Crystal and magnetic structures of layer transition metal phosphate hydrates. *Inorg. Chem.* **34**, 3917–3927.
- Carling, S. G., Mathonière, C., Day, P., Malik, K. M. A., Coles, S. J. & Hursthouse, M. B. 1996 Crystal structure and magnetic properties of the layer ferrimagnet $N(n-C_5H_{11})_4Mn^{II}Fe^{III}(C_2O_4)_3$. *J. Chem. Soc. Dalton Trans.*, pp. 1839–1844.
- Carlino, S. 1997 The intercalation of carboxylic acids into layered double hydroxides: a critical evaluation and review of the different methods. *Solid State Ionics* **98**, 73–84.
- Chikazumi, S. 1978 *Physics of magnetism*. Wiley.
- Clearfield, A. (ed.) 1991 *Inorganic ion exchange materials*. Boca Raton, FL: CRC.
- Clemente-Leon, M., Coronado, E., Galan-Mascaros, J.-R. & Gomez-Garcia, C. 1997 Intercalation of decamethylferrocenium cations in bimetallic oxalate-bridged two-dimensional magnets. *Chem. Commun.*, pp. 1727–1728.
- Cotton, F. A., Lin, C. & Murillo, C. A. 1998 Coupling Mo_2^{n+} units via dicarboxylate bridges. *J. Chem. Soc. Dalton Trans.*, pp. 3151–3153.
- Day, P. 1988 Nickel dibromide: a magnetic detective story. *Acc. Chem. Res.* **211**, 250–254.
- Day, P. 1997 Coordination complexes as organic–inorganic layer magnets. *J. Chem. Soc. Dalton Trans.*, pp. 701–705.
- Decurtins, S., Ferlay, S., Pellaux, R., Gross, M. & Schmalle, 1998 Examples of supramolecular coordination compounds and their supramolecular functions. In *Supramolecular engineering of synthetic metallic materials* (ed. J. Veciana, C. Rovira, C. & D. B. Amabilino), NATO ASI C518, pp. 175–196. Dordrecht: Kluwer.
- De Jongh, L. J. (ed.) 1990 *Magnetic properties of layered transition metal compounds*. Dordrecht: Kluwer.

- De Jongh, L. J. & Miedema, A. R. 1974 Experiments on simple magnetic model systems. *Adv. Phys.* **23**, 1–260.
- De Jongh, L. J., Botterman, A. C., De Bose, F. R. & Miedema, A. R. 1969 Transition temperature of the two dimensional Heisenberg ferromagnet with $s = \frac{1}{2}$. *J. Appl. Phys.* **40**, 1363–1365.
- Drillon, M. & Panissod, P. 1998 Long range ferromagnetism in hybrid compounds: the role of dipolar interactions. *J. Mag. Mag. Mater.* **188**, 93–99.
- Fair, M. J., Gregson, A. K., Day, P. & Hutchings, M. T. 1977 Neutron scattering study of the magnetism of Rb_2CrCl_4 , a two dimensional easy-plane ferromagnet. *Physica B* **86–88**, 657–659.
- Fanucci, G. E., Nixon, C. M., Petruska, M. A., Seip, C. T., Talham, D. R., Granroth, G. E. & Meisel, M. W. 1998 Metal phosphonate Langmuir–Blodgett films: monolayers and organic/inorganic dual network assemblies. In *Supramolecular engineering of synthetic metallic materials* (ed. J. Veciana, C. Rovira & D. B. Amabilino). NATO ASI C518, pp. 465–475. Dordrecht: Kluwer.
- Figgis, B. N. 1966 *Introduction to ligand fields*. London: Wiley-Interscience.
- Fogg, A. M., Dunn, J. S. & O'Hare, D. 1998a Formation of second-stage intercalation reactions of the layered double hydroxide $[\text{LiAl}_2(\text{OH})_6]\text{Cl} \cdot \text{H}_2\text{O}$ as observed by time-resolved *in situ* X-ray diffraction. *Chem. Mater.* **10**, 356–360.
- Fogg, A. M., Dunn, J. S., Shyu, S.-G., Cary, D. R. & O'Hare, D. 1998b Selective ion exchange intercalation of isomeric dicarboxylate anions into the layered double hydroxide $[\text{LiAl}_2(\text{OH})_6]\text{Cl} \cdot \text{H}_2\text{O}$. *Chem. Mater.* **10**, 351–355.
- Fujita, W. & Awaga, K. 1996 Magnetic properties of $\text{Cu}_2(\text{OH})_3(\text{alkanecarboxylate})$ compounds: drastic modification with extension of the alkyl chain. *Inorg. Chem.* **35**, 1915–1917.
- Goodenough, J. B. 1963 *Magnetism and the chemical bond*. Wiley.
- Heinrich, B. & Bland, J. A. C. 1994 *Ultrathin magnetic structures*. Springer.
- Herpin, A. 1968 *Théorie du Magnétisme*. Paris: Presse Universitaire de France.
- Jacobsen, A. J. 1992 Intercalation reactions of layered compounds. In *Solid state chemistry: compounds* (ed. P. Day & A. Cheetham). Oxford University Press.
- Jones, E. R. & Stone, J. A. 1972 Metamagnetism in neptunium(V) oxalate. *J. Chem. Phys.* **56**, 1343–1347.
- Kahn, O. 1993 *Molecular magnetism*. New York: VCH.
- Kahn, O. (ed.) 1996 *Magnetism: a supramolecular function*. NATO ASI series C484. Dordrecht: Kluwer.
- Kurmoo, M. & Kepert, C. J. 1998 Hard magnets based on transition metal complexes with the dicyanamide anion, $\{\text{N}(\text{CN})_2\}^-$. *New J. Chem.*, pp. 1515–1524.
- Kurmoo, M., Graham, A. W., Day, P., Coles, S. J., Hursthouse, M. B., Caulfield, J. L., Singleton, J., Pratt, F. L., Hayes, W., Ducasse, L. & Guionneau, P. 1995 Superconducting and semiconducting magnetic charge transfer salts: $(\text{BEDT-TTF})_4\text{AFe}(\text{C}_2\text{O}_4)_3 \cdot \text{C}_6\text{H}_5\text{CN}$ ($\text{A} = \text{H}_2\text{O}$, K, NH_4). *J. Am. Chem. Soc.* **117**, 12 209–12 217.
- Kurmoo, M., Day, P., Derory, A., Estournès, C., Poinso, R., Stead, M. J. & Kepert, C. J. 1999 3D-long range magnetic ordering in layered metal-hydroxide triangular lattices 25 Å apart. *J. Solid State Chem.* **145**, 452–459.
- Laget, V., Rouba, S., Rabu, P., Hornick, C. & Drillon, M. 1996 Long range ferromagnetism in tunable cobalt(II) layered compounds up to 25 Å apart. *J. Mag. Mag. Mater.* **154**, L7–L11.
- Laget, V., Hornick, C., Rabu, P., Drillon, M. & Ziessel, R. 1998 Molecular magnets hybrid organic-inorganic layered compounds with very long-range ferromagnetism. *Coord. Chem. Rev.* **178–180**, 1533–1553.
- Lever, A. P. B. 1986 *Inorganic electronic spectroscopy*. Elsevier.

- Li, H., Eddouadi, M., Groy, T. L. & Yaghi, O. M. 1998 Establishing microporosity in open metal-organic frameworks: gas sorption isotherms for Zn(BDC) (BDC = 1,4-benzenedicarboxylate). *J. Am. Chem. Soc.* **120**, 8571–8572.
- Louer, M., Louer, D. & Grandjean, D. 1973 Etude structurale des hydroxynitrates de nickel et de zinc. I. Classification structurale. *Acta Crystallogr. B* **29**, 1696–1710.
- Mabbs, F. E. & Machin, D. J. 1973 *Magnetism and transition metal complexes*. London: Chapman & Hall.
- Mathonière, C., Nuttall, C. J., Carling, S. G. & Day, P. 1996 Ferrimagnetic mixed-valency and mixed-metal tris(oxalato)iron(III) compounds: synthesis, structure and magnetism. *Inorg. Chem.* **35**, 1201–1206.
- Meyn, M., Beneke, K. & Lagaly, G. 1993 Anion exchange reactions of hydroxy double salts. *Inorg. Chem.* **32**, 1209–1215.
- Miedema, A. R., van Kempen, H. & Huiskamp, W. J. 1963 Experimental study of the simple ferromagnetism in $\text{CuK}_2\text{Cl}_4 \cdot 2\text{H}_2\text{O}$ and $\text{Cu}(\text{NH}_4)_2\text{Cl}_4 \cdot 2\text{H}_2\text{O}$. *Physica* **29**, 1266–1280.
- Mitchell, I. V. 1990 *Pillared layered structures: current trends and applications*. Elsevier.
- Nagamiya, T., Yosida, K. & Kubo, R. 1955 Antiferromagnetism. *Adv. Phys.* **4**, 1–112.
- Nakamoto, K. 1986 *Infrared and Raman spectra of inorganic and coordination compounds*, p. 230. Wiley.
- Newman, S. P. & Jones, W. 1998 Synthesis, characterization and applications of layered double hydroxides containing organic guests. *New J. Chem.* **22**, 105–115.
- Nicoud, J.-F. 1994 Towards new multi-property materials. *Science* **63**, 636–637.
- Nuttall, C. J. & Day, P. 1998 Magnetization of the layer compounds $\text{AFe}^{\text{II}}\text{Fe}^{\text{III}}(\text{C}_2\text{O}_4)_3$ (A = organic cation), in low and high magnetic fields: manifestation of Néel N- and Q-type ferrimagnetism in a molecular lattice. *Chem. Mater.* **10**, 3050–3057.
- O'Hare, D. 1993 Inorganic intercalation chemistry. In *Inorganic materials* (ed. D. W. Bruce & D. O'Hare). London: Wiley.
- Rabu, P., Angelov, S., Legoll, P., Belaiche, M. & Drillon, M. 1993 Ferromagnetism in triangular cobalt(II) layers: comparison of $\text{Co}(\text{OH})_2$ and $\text{Co}_2(\text{NO}_3)(\text{OH})_3$. *Inorg. Chem.* **32**, 2463–2468.
- Rodriguez-Carvajal, J. 1997 *FullProf: short reference guide to the program*, edn 3.2. Paris: CEA-CNRS.
- Rouba, S. 1996 Corrélations structures-propriétés magnetiques dans une série d'hydroxynitrate de métaux de transition 1d et 2d. Thèse doctorat, Université Louis Pasteur, Strasbourg, France.
- Schollhorn, R. 1984 *Intercalation compounds*. London: Academic.
- Schieber, M. M. 1967 *Experimental magnetochemistry, selected topics in solid state physics* (ed. E. P. Wohlfarth), vol. VIII. North-Holland.
- Stählin, W. & Oswald, H. R. 1970 The crystal structure of zinc hydroxide nitrate, $\text{Zn}_5(\text{OH})_8(\text{NO}_3)_2(\text{H}_2\text{O})_2$. *Acta Crystallogr. B* **26**, 860–863.
- Stählin, W. & Oswald, H. R. 1971 The infrared spectrum and thermal analysis of zinc hydroxide nitrate. *J. Solid State Chem.* **2**, 252–255.
- Stryjewski, E. & Giordano, N. 1977 Metamagnetism. *Adv. Phys.* **26**, 487–650.
- Takada, T., Bando, Y., Kiyama, M. & Mitamoto, K. 1966a The magnetic property of $\beta\text{-Co}(\text{OH})_2$. *J. Phys. Soc. Jap.* **21**, 2726.
- Takada, T., Bando, Y., Kiyama, M., Mitamoto, K. & Sato, T. 1966b The magnetic property of $\text{Ni}(\text{OH})_2$. *J. Phys. Soc. Jap.* **21**, 2745.
- Tamaki, H., Mitsumi, M., Nakamura, K., Matsumoto, N., Kida, S., Okawa, H. & Iijima, S. 1992a Metal-complex ferrimagnets with the formula $\{\text{NBu}_4[\text{M}(\text{II})\text{Fe}(\text{III})(\text{ox})_3]\}_\infty$ (NBu_4^+ = tetra(*n*-butyl)ammonium ion, ox^{2-} = oxalate ion, $\text{M} = \text{Fe}^{2+}, \text{Ni}^{2+}$). *Chem. Lett.*, pp. 1975–1978.
- Tamaki, H., Zhong, Z. J., Matsumoto, N., Kida, S., Koikawa, M., Achiwa, N., Hashimoto, Y. & Okawa, H. 1992b *J. Am. Chem. Soc.* **114**, 6974.

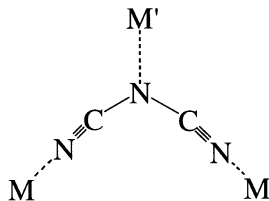
- Wells, A. F. 1984 *Structural inorganic chemistry*. Oxford University Press.
- Werner, P. E., Eriksson, L. & Westdahl, M. 1985 A semi-exhaustive trial-and-error powder indexing program for all symmetries. *J. Appl. Crystallogr.* **18**, 367–370.
- Zotov, N., Petrov, K. & Dimitova-Pankova, M. 1990 Infrared spectra of Cu(II)–Co(II) mixed hydroxide nitrates. *J. Phys. Chem. Solids* **51**, 1199–1205.

Discussion

B. J. BUSHBY (*School of Chemistry, University of Leeds, UK*). Some of Dr Kurmoo's data on finely divided crystals suggest that we are approaching a mono-domain structure. Given the size of the crystals, what does this imply regarding the number of spins in a domain? Is this a reasonable figure, and, indeed, what sizes do we expect for domains in molecular systems?

M. KURMOO. Domain size is an important parameter, among others including exchange and anisotropy energies and form of the samples, when quoting coercive field. The samples presented, showing magnetic behaviour approaching single domain, were elongated plates of maximum dimension of *ca.* 100 nm. This translates to *ca.* 10^6 magnetic centres. This is larger than those of metallic particles, which are of the order of 25 nm, and is close to those of oxides. In my opinion, the domain size will increase when the exchange energy decreases and will decrease when the anisotropy energy increases. Therefore, it depends on the particular system and on the single-ion anisotropy and shape of the particles.

M. VERDAGUER (*Laboratoire de Chimie Inorganique et Matériaux Moléculaires, Université Pierre et Marie Curie, Paris, France*). The dicyanamide ligand has two different coordination sites. Did Dr Kurmoo try (and did he succeed) to get structurally ordered bimetallic systems such as



M. KURMOO. The dicyanamide contains three nitrogen atoms and two different coordination sites (two nitrile and one amide). Yes, it would be of interest to prepare structurally ordered bimetallic systems, but we have not yet tried this. The method of preparation of the binary compounds, $M(N(CN)_2)_2$, is a one-pot procedure.

